EDGEWOOD CHEMICAL BIOLOGICAL CENTER
U.S. ARMY RESEARCH, DEVELOPMENT AND ENGINEERING COMMAND
Aberdeen Proving Ground, MD 21010-5424

ECBC-TR-1550

MATRIX-FREE ASSISTED LASER DESORPTION IONIZATION USING METAL-ORGANIC FRAMEWORKS

Rabih E. Jabbour
Gregory Peterson
Jared DeCoste

RESEARCH AND TECHNOLOGY DIRECTORATE

Yousef Jabaji

University of Maryland-Baltimore County
Baltimore, MD 21250-0001

January 2019

Disclaimer

The findings in this report are not to be construed as an official Department of the Army position unless so designated by other authorizing documents.

REPORT DOCUMENTATION PAGE

Form Approved
OMB No. 0704-0188

1. REPORT DATE *(DD-MM-YYYY)*	2. REPORT TYPE	3. DATES COVERED *(From - To)*
XX-01-2019	Final	Oct 2016–Sep 2018

4. TITLE AND SUBTITLE
Matrix-Free Assisted Laser Desorption Ionization Using Metal-Organic Frameworks

5a. CONTRACT NUMBER

5b. GRANT NUMBER

5c. PROGRAM ELEMENT NUMBER

6. AUTHOR(S)
Jabbour, Rabih E.; Peterson, Gregory; DeCoste, Jared (ECBC); and Jabaji, Yousef (UMBC)

5d. PROJECT NUMBER
PE 0601102A Project VR9

5e. TASK NUMBER

5f. WORK UNIT NUMBER

7. PERFORMING ORGANIZATION NAME(S) AND ADDRESS(ES)
Director, ECBC, ATTN: RDCB-DRI-D//DRP-F, APG, MD 21010-5424
University of Maryland-Baltimore County (UMBC), Engineering Department; 1000 Hilltop Cir, Baltimore, MD 21250-0001

8. PERFORMING ORGANIZATION REPORT NUMBER
ECBC-TR-1550

9. SPONSORING / MONITORING AGENCY NAME(S) AND ADDRESS(ES)
Defense Threat Reduction Agency; 8725 John J. Kingman Road, MSC 6201, Fort Belvoir, VA 22060-6201

10. SPONSOR/MONITOR'S ACRONYM(S)
DTRA; U.S. Army in-House SSI

11. SPONSOR/MONITOR'S REPORT NUMBER(S)

12. DISTRIBUTION / AVAILABILITY STATEMENT
Approved for public release: distribution unlimited.

13. SULEMENTARY NOTES

14. ABSTRACT:
We studied the ionization mechanism and determined the factors that affect the charge-transfer process during matrix-assisted laser desorption/ionization mass spectrometry (MALDI-MS). We addressed the binding affinity issue between metal-organic frameworks (MOFs) and analytes using low-frequency Raman spectroscopy (LFRS) to determine inter- and intramolecular changes between crystalline and amorphous states of MOFs with different analytes. These analytes were classified as acidic or basic compounds. As soon as we understand the basic properties of MOF/analyte mixtures, we will investigate how to design MOFs that can enhance ionization efficiency for a wide range of compounds during MALDI-MS analysis. This knowledge will be used to design and develop a reliable, functionalized MOF substrate that can desorb biomolecules and selectively capture analytes of interest. We addressed the potential inter- and intramolecular changes for MOF/analyte mixtures using LFRS and MALDI-MS techniques. The MOFs used in the LFRS were UiO-66-COOH and UiO-66-NH_2, and the analytes were pyridine, benzoic acid, cytidine, lauric acid, and guanine. More MOFs than those tested by the LFRS technique were used for the MALDI-MS analyses. Most of the MOFs were obtained from internal sources, either through synthesis or by leveraging from already-funded projects that use MOFs.

15. SUBJECT TERMS
Metal-organic framework (MOF)
Low-frequency Raman spectroscopy (LFRS)
Matrix-assisted laser desorption/ionization mass spectrometry (MALDI-MS)
Detection
Identification
Biothreats

16. SECURITY CLASSIFICATION OF:			17. LIMITATION OF ABSTRACT	18. NUMBER OF PAGES	19a. NAME OF RESPONSIBLE PERSON
a. REPORT	b. ABSTRACT	c. THIS PAGE			Renu B. Rastogi
U	U	U	UU	28	19b. TELEPHONE NUMBER *(include area code)* (410) 436-7545

Blank

PREFACE

The work described in this report was authorized under project number PE 0601102A Project VR9. The work was started in October 2016 and completed in September 2018.

The use of either trade or manufacturers' names in this report does not constitute an official endorsement of any commercial products. This report may not be cited for purposes of advertisement.

This report has been approved for public release.

Acknowledgments

The authors acknowledge the following individuals for their hard work and assistance with the execution of this technical program:

- Dr. A. Way Fountain for his guidance and management of the Basic Research Program at U.S. Army Edgewood Chemical Biological Center (ECBC; Aberdeen Proving Ground [APG], MD).
- Drs. Ashish Tripathi and Erik Emmons for their technical and experimental support (ECBC).
- Dr. Robert DiTargiani for facilitating the use of the matrix-assisted laser desorption/ionization mass spectrometry system at the U.S. Army Medical Research Institute of Chemical Defense (APG, MD).

Blank

CONTENTS

FIGURES

MATRIX-FREE ASSISTED LASER DESORPTION IONIZATION USING METAL-ORGANIC FRAMEWORKS

1. INTRODUCTION

Matrix-assisted laser desorption/ionization (MALDI) is a soft ionization technique that is widely applied in the characterization of large biomolecules using various mass spectrometry (MS) analyzers, specifically, time-of-flight (TOF) analyzers.[1–4] The MALDI process involves the deposition of an analyte solution onto a metal substrate before the addition of a matrix.[5] The matrix/analyte dry spot is exposed to a UV laser, and the laser energy that is absorbed by the matrix/analyte is converted into heat energy that initiates charge transfer, which results in the desorption of the matrix and analyte molecules in ionized form. The positive ions are then accelerated through a vacuum into MS analyses. However, the MALDI process lacks guiding systematic principles, which has resulted in mostly empirical work. For example, there is no universal matrix that can be used in the MALDI-MS analysis of biomolecules. Hundreds of compounds were assessed with several analytes and were given qualitative ratings.[6–8] These variables were the products of differences in charge transfer efficiency between the matrix and analytes because of chemical and structural factors.[7]

This problem represents an urgent analytical need that can advance the MALDI process toward mechanistic understanding. Metal-organic frameworks (MOFs) are an emerging class of porous materials that have been studied in multiple areas, including gas storage,[9,10] sensing,[11] air purification,[12] and catalysis.[13] MOFs are typically synthesized from metal oxide secondary building units (SBUs) connected by organic linkers to form a reticulated, porous network. MOFs are used because of their versatility and thermal stability. The unique physical and chemical properties of MOFs provide the potential to serve as MALDI matrixes that are capable of ionizing a wide range of analytes. However, because of their structural complexity, we first attempted to determine the existence of any interaction between the analytes and the MOFs when they were mixed together. We used low-frequency Raman spectroscopy (LFRS) to determine the inter- and intramolecular changes between free MOFs. In addition, LFRS was used to investigate the reactions that resulted from mixing analytes in an amorphous environment.[1–16] LFRS is a developing technique that concurrently provides vibrational spectra for tested compounds in the terahertz and normal Raman spectral regions, which are indicative of any potential physical and chemical changes in a given analyte. The LFRS process provides a wealth of information about material properties in a fast and non-destructive manner. In the case of MOFs, LFRS can be used to investigate the binding properties of MOFs with the analytes of interest and to determine the nature of such binding.

Currently, there are two different mechanisms that explain the ionization process in MALDI-MS analysis. The first mechanism is based on the coupled chemical and physical dynamics model, which involves charge transfer during the excitation stage of a matrix/analyte mixture, resulting from exposure to laser power.[17] The second mechanism is based on a cluster model, which involves a combination of proton and intracluster charge transfer during the desolvation step of the MALDI process.[18] Accordingly, we designed our experimental approach for MOF/analyte interaction during the MALDI process to determine the ionization model that

governs the ionization step. This report addresses the results of these mechanistic-oriented experiments to help us determine the basic elements that contribute to the MALDI ionization process of the MOF/analyte mixtures. This base knowledge will aid in the development of efficient matrix-free desorption substrates for MS analyses. MOF materials have demonstrated superior homogenous and heterogeneous catalysis characteristics that will be transcribed to the MALDI process. Moreover, the diversity of MOFs can be envisioned to act as a selective desorption surface for specific groups of analytes without reliance on the addition of external reagents.

The overall goal of this project was to study the mechanism of ionization and to determine the influence of factors that affect the charge-transfer process during the MALDI-MS ionization. We also addressed the binding affinity issue between MOFs and analytes using the LFRS technique to research inter- and intramolecular changes between the MOF crystalline and amorphous states with different analytes. These analytes were classified as acidic or basic compounds. As soon as we understand the basic properties of the MOF/analyte mixture, we will be able to determine how to design MOFs that can enhance the ionization efficiency for a wide range of compounds during MALDI-MS analysis. This information will be used to design and develop a reliable, functionalized MOF substrate that can desorb biomolecules and selectively capture the analytes of interest.

This study addressed the potential intra- and intermolecular changes for MOF/analyte mixtures using LFRS and MALDI-MS techniques. The MOFs used in the LFRS technique were UiO-66-COOH and UiO-66-NH_2, and the analytes were pyridine, benzoic acid, cytidine, lauric acid, and guanine. More MOFs than those tested by the LFRS technique were used for the MALDI-MS analyses. Most of the MOFs were obtained from internal sources, either through synthesis or by leveraging from already-funded projects that utilize MOFs. The structures for some of the MOFs and analytes are shown in Figure 1.

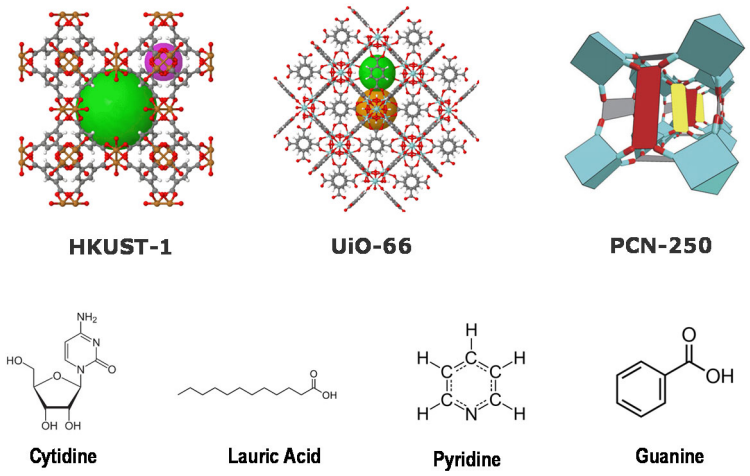

Figure 1. Representative MOFs including HKUST-1 (named for Hong Kong University of Science and Technology), modified UiO-66 with –COOH and –NH_2 functional groups, and poly-coordinated network (PCN)-250 MOFs. The ball embedded in the MOF structures represents the relative pore sizes that are found within the structure of the MOFs. The analytes shown are cytidine, lauric acid, pyridine, and guanine.

2. MATERIALS AND METHODS

2.1 MOF Network Synthesis

Various MOFs with different porosity and linker groups were used in this research to determine their performance during the MALDI-MS process. The selected MOFs were UiO-66, UiO-66-COOH, UiO-66-NH_2, copper(II) benzene-1,3,5-tricarboxylate (Cu-BTC/HKUST-1), PCN-250, PCN-250-Ni, and MOF-545 with different metal ions. All of these MOFs were synthesized elsewhere using the methods reported in the literature.[19–21] Briefly, the synthesis of UiO-66-NH_2 was performed by dissolving 1.5 g of $ZrCl^4$ and 1.5 g of 2-amino-1,4-benzene dicarboxylic acid in 180 mL of dimethylformamide at room temperature in a volumetric flask. The resulting mixture was preheated in an oven at 80 °C for 12 h and then held at 100 °C for 24 h. After cooling to room temperature in air, the resulting solid was filtered and repeatedly washed with absolute ethanol for 3 days at 60 °C in a water bath. The resulting yellow powder was filtered and transferred for drying under vacuum at room temperature. All the tested MOF substrates were characterized and validated using appropriate techniques to ensure the formation of the desired chemical network and determine the surface coverage area, pore size, and volume.[22,23]

2.2 LFRS Measurements

The low-frequency Raman scattering from an MOF sample was measured in Stokes and anti-Stokes vibrational spectra. The Raman spectroscopy experiments were performed using a WITec alpha300 R confocal Raman microscopy system (WITec Instruments Corporation; Knoxville, TN). A 100× microscope objective in the Raman microscopy was used, and a Rayshield (Tempe, AZ) notch filter was used to generate LFRS features from a wavenumber of 10 cm^{-1}. The solid-state laser that was used had a wavelength of 532.1 nm, and a wavelength of 532 nm with a power of ∼2 mW incident on the substrate was used for excitation. The Raman-scattered light was collected in the backscattering configuration and transmitted through a 100 μm slit to a 600 grooves/mm grating, which dispersed the light onto a thermoelectrically cooled charge-coupled device camera (WITec DV401 A). A spectral resolution of approximately 5 cm^{-1} was obtained. Spectra were acquired with 5–10 s acquisition times. At a lower Raman shift, spurious contributions from the elastic line can be detected by measuring the scattering from a metal surface. On the anti-Stokes side, our spectrometer instrument response was better, which allowed us to measure the Raman spectrum down to 5 cm^{-1} of the Raman shift. The sample image in the entrance spectrometer plane was selected in such a way that the contribution from the glassy slide did not come into the spectrometer. No polarization selection was used.

2.3 MOF as a Matrix for MALDI-MS Analysis

The standard sample preparation protocol for conventional MALDI-MS was used to perform all of the analyses. Briefly, mass spectra were recorded with a MALDI Synapt G2-S high-definition mass spectrometer (Waters; Milford, MA). The buffer gas was adjusted using the default gas line connected to the hexapole ion guide compartment. Standard MALDI matrices and an analyte kit were purchased from Sigma-Aldrich (St. Louis, MO). The kit contains 1 mg of

cinnamic acid (CA), 1 mg of 98% sinapic acid (SA), 4,6-dinitrophloroglucinol (97%), insulin (from bovine pancreas), ubiquitin (from bovine erythrocytes), and carbonic anhydrase (from bovine erythrocytes). Each kit also contained a sufficient amount of MALDI solvent composed of acetonitrile (ACN), high-performance liquid chromatography-grade water, and trifluoroacetic acid (TFA). The high-performance liquid chromatography-grade methanol (MeOH) and water were purchased from Thermo Fisher Scientific, Inc. (Waltham, MA).

A saturated solution of the matrices was prepared at a concentration of 1 μg/mL and dissolved in 50:50:0.1% ACN/water/TFA for CA and SA. The standard calibration analytes supplied in the MALDI kit were diluted in the same solvent composition as that of the MALDI matrix. A MALDI target plate was spotted with 1–2 μL of the samples using a stacking or mixing approach. The stacking approach consisted of spotting 1 μL of the matrix solution on the MALDI plate, allowing the solution to dry, and then re-spotting the plate with 1 μL of the analyte solution.

We followed the conventional MALDI spotting approach in which a 1:10 ratio of analytes/matrix is mixed before it is spotted on the MALDI substrate. We spotted 1–2 μL of mixture on the MALDI target plate and allowed it to dry before we inserted the plate into the MALDI instrument. The same sample preparation protocol used in the conventional MALDI setup was also used with the tested MOFs. Every MOF/analyte mixture was spotted in triplicate on the MALDI target plate and allowed to dry before MS analysis was performed.

The Waters mass spectrometer was equipped with a commercial MALDI source and operated with an Nd:YAG laser (355 nm and 200 Hz, respectively). Mass spectral acquisitions were performed in positive ion mode using the following MALDI settings: 0 V on the sample plate holder, 10 V for extraction, 350 V for hexapole, and 10 V for aperture. The laser power was set at 250 amu for 25–50 % laser fluence at a 200 Hz firing rate. The sample plate voltage was held at 10 kV. Calibration was performed using polyethylene glycol adducts between 300 and 3000 mass-to-charge ratios (*m/z*).

The mass spectra were acquired using the reflectron positive ion mode with a reflectron voltage of 18 kV and an ion source lens voltage of 10 kV. The laser repetition rate was set at 20 Hz, and increments of 20 laser shots were used to acquire the mass spectrum with a total of 100 shots per each mass spectrum. The MALDI instrument vendor software was used to process the data and to obtain the MALDI mass spectra of the studied MOFs.

3. RESULTS AND DISCUSSIONS

3.1 Effect of Functional Groups on the LFRS Analysis of UiO-66-COOH Complexes

LFRS was used to study the potential chemical and physical changes when the UiO-66-COOH was mixed with different acidic and basic analytes. The mixture was suspended in water and vortexed for 20 min. The mixture was then centrifuged, and the supernatant and pellet were aliquoted and deposited on aluminum oxide slides before LFRS analysis was

conducted. Figure 2 shows the LFRS spectra for UiO-66-COOH and its mixture with benzoic acid, lauric acid, cytidine, and guanine. The LFRS results showed subtle differences in the spectral signatures for the MOF/analyte mixtures in the normal Raman and terahertz regions. There is a Raman shift band for the UiO-66-COOH/cytidine mixture at 954 cm^{-1} that is unique and was not found in the spectra of the other UiO-66-COOH mixtures. The Raman spectral data also revealed different shifts for acidic and basic compounds, as reflected by the increased intensity for Raman shift signals in the regions of 720, 954, and 1010 cm^{-1}. Based on these LFRS data, we observed that cytidine, guanine, and benzoic acid have certain chemical interactions with UiO-66-COOH.

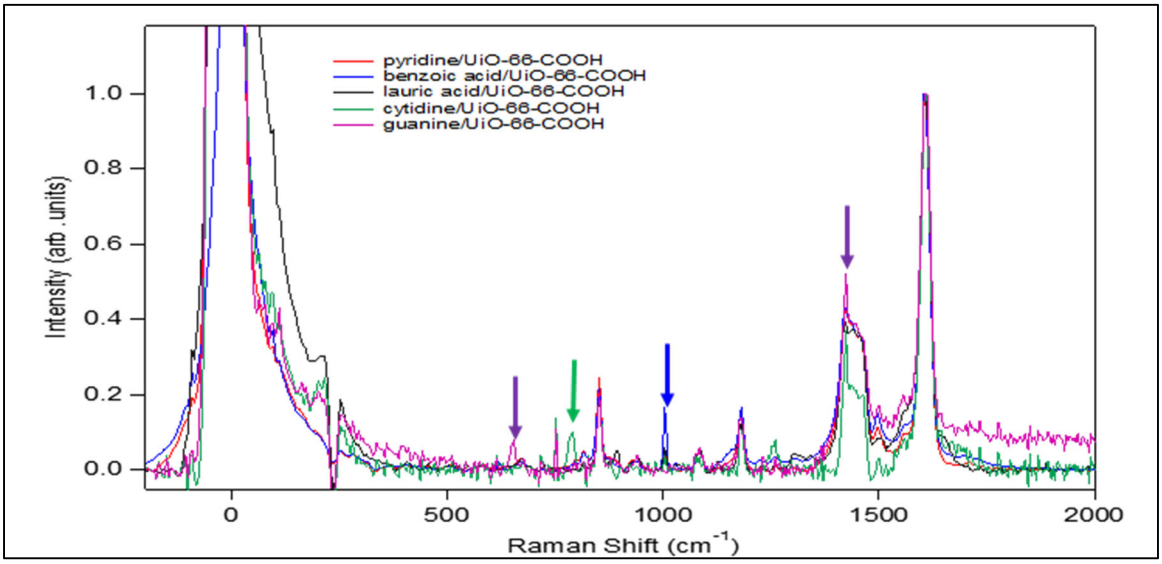

Figure 2. LFRS spectra for UiO-66-COOH and different analytes. All samples were mixed with UiO-66-COOH. LFRS results are stacked.

The terahertz data showed a loss of crystalline structure at around the 0 cm^{-1} Raman shift, which indicates a physical change to the structure of the UiO-66-COOH when it was mixed with analytes. This observation was further investigated by LFRS analyses of pure UiO-66-COOH and its mixture with benzoic acid (Figure 3). The LFRS data showed that benzoic acid is crystalline in its pure state, whereas it has amorphous features when mixed with UiO-66-COOH. This subtle difference in the terahertz region supports the observation seen in the Raman shift for the UiO-66-COOH interaction with different analytes in which all of these mixtures showed loss of crystalline structure, as evident by loss of Stoke and anti-Stoke peaks in the terahertz region.

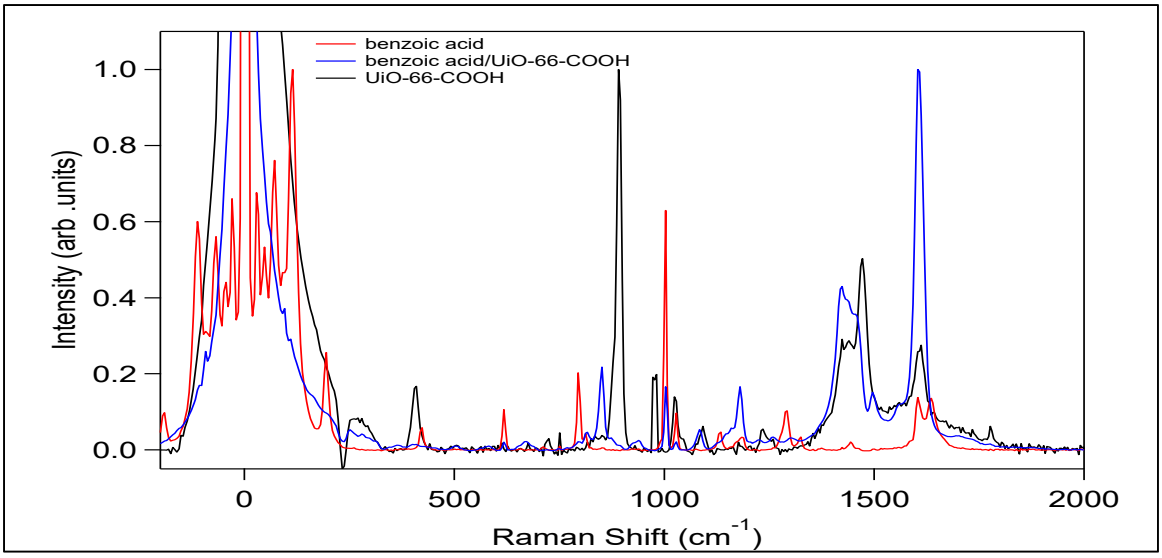

Figure 3. LFRS spectra for UiO-66-COOH, benzoic acid, and UiO-66-COOH and benzoic acid mixture.

In Figure 3, the Raman vibrational band shift that was observed when pure UiO-66-COOH was compared with UiO-66-COOH/benzoic acid mixture shows the strong interaction between benzoic acid and UiO-66-COOH. It is noteworthy to mention that the normal Raman spectral features of pure benzoic acid differ from the normal Raman spectral features of UiO-66-COOH-benzoic acid. However, some common vibrational Raman bands were seen in the pure benzoic acid and UiO-66-COOH-benzoic acid mixture. Overall, the LFRS analysis of UiO-66-COOH and the acids and bases indicated some acid/base chemistry taking place, as shown by the more observable changes with the basic compounds, and to a lesser extent, with the acidic compounds. New vibrational bands for the basic compounds appeared in the normal Raman shift region as compared with only the enhancement of common features for the acidic compounds in the same spectral region.

3.2 Effect of Functional Groups on the LFRS Analysis of UiO-66-NH_2 Complexes

LFRS analysis was also used to characterize the potential interaction of the UiO-66-NH_2 with the studied analytes. The LFRS procedure mentioned in Section 3.1 was used. In this part of the study, the UiO-66-NH_2 was a modified UiO-66 structure with the addition of the benzyl amine group as an active site on the MOF surface for potential interaction with the analyte molecules. The LFRS analysis produced a large number of fluorescent signals in the background for the UiO-66-NH_2 that required longer photobleaching times before data collection. The mixtures of UiO-66-NH_2 and guanine, lauric acid, or cytidine showed a dominant vibrational saturation that overloads normal Raman vibrational bands and therefore are not included in this discussion. The LFRS results that showed satisfactory signal-to-noise ratio responses were the mixtures of UiO-66-NH_2 with pyridine or benzoic acid.

LFRS spectra of pure pyridine and benzoic acid suspended in pure water solution were acquired. These LFRS results are shown in Figure 4. Benzoic acid and pyridine have

several vibrational bands that are different in their respective normal Raman and terahertz spectral regions. Benzoic acid has sharp vibrational bands in the terahertz region, whereas these bands are absent from the LFRS spectrum of pyridine. This is indicative of the different structures of these two compounds. Benzoic acid preserves its crystallinity, as evident by the sharp terahertz spectral peaks, whereas pyridine does not. Moreover, the vibrational bands in the normal Raman region show that there are shifts between the common features for the two compounds. The C=C stretch band at 1620 cm^{-1} for pyridine has a higher intensity and is shifted by several inverse centimeters (cm^{-1}) for benzoic acid. However, the aromatic band at 1000 cm^{-1} is the same for both but with a higher intensity for pyridine than for benzoic acid.

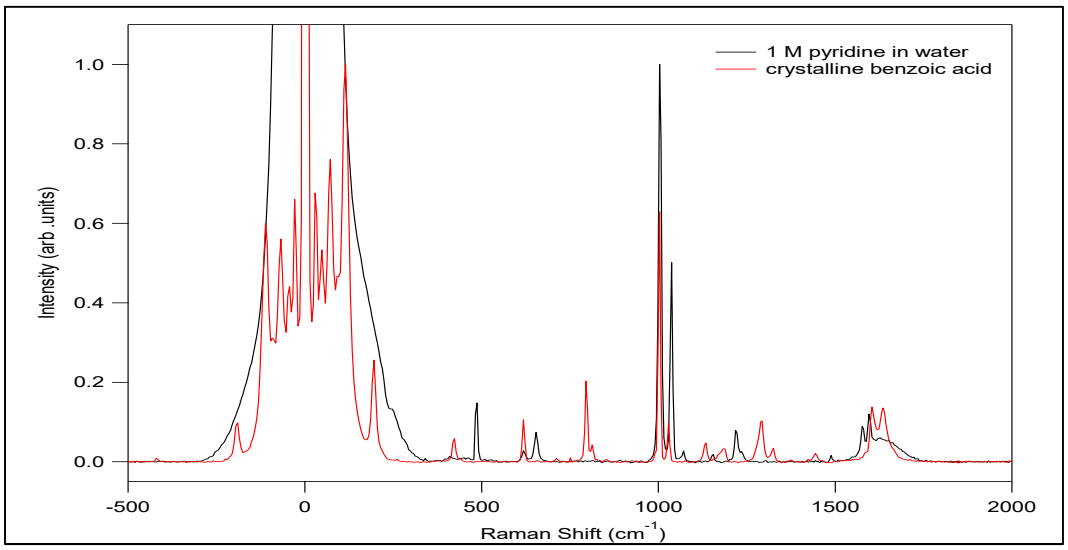

Figure 4. LFRS spectra comparing the normal Raman and terahertz regions for pure pyridine and benzoic acid suspended in water.

When one of these analytes was mixed with UiO-66-NH_2, there was a shift for both in the normal and terahertz regions of the Raman spectra, as shown in Figure 5, which presents the LFRS spectra for the UiO-66-NH_2/pyridine and UiO-66-NH_2/benzoic acid mixtures. After each analyte was mixed with UiO-66-NH_2, the normal Raman spectra for both compounds had different vibrational band changes. The aromatic band for pyridine at 1000 cm^{-1} was reduced as compared with that of benzoic acid. In addition, there was a loss of crystallinity for benzoic acid when it was mixed with UiO-66-NH_2 as compared with the terahertz spectral signature of the pure compound. This is indicative of structural changes that could be the result of interactions between the analyte molecules and UiO-66-NH_2. Moreover, the change in the normal Raman supports this assumption because of the different vibrational bands that changed for the two compounds. This change indicates the alteration of the molecular structure of the analyte when it was mixed with UiO-66-NH_2.

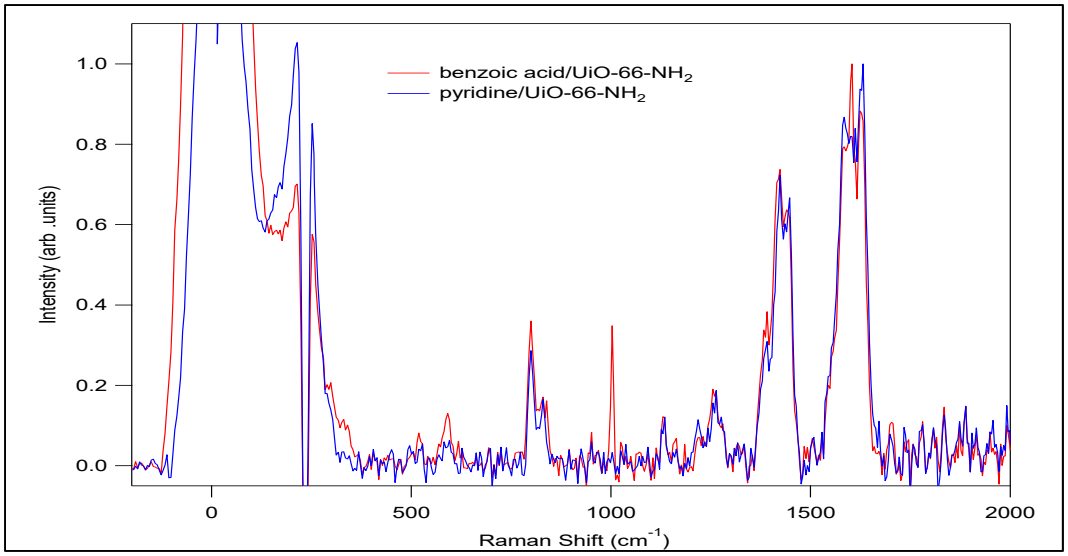

Figure 5. LFRS spectra comparing the normal Raman and terahertz regions for pure pyridine and benzoic acid suspended with UiO-66-NH_2 MOF in pure water.

Overall, the LFRS analysis showed that differing degrees of chemical and physical changes exist for the studied compounds when they are mixed with different MOFs. The MOF itself has subtle Raman spectral signatures and characteristics that need to be addressed in a separate study, such as the differing degree of fluorescence for amine-modified UiO-66 as compared with that of the carboxylic acid modification of the same base MOF structure. It is worth mentioning that a high fluorescence level of UiO-66-NH_2 was also observed when fluorescence emission spectroscopy was used.

3.3 Effect of Functional Groups of MOFs on the MALDI-MS Analysis of Acidic and Basic Compounds

MALDI-MS analyses were performed on mixtures of UiO-66, UiO-66-COOH, and UiO-66-NH_2 with the same analytes that were used in the LFRS spectral analyses. Different mixtures of the MOFs were prepared, as described in Section 2, and 1 µL of mixture suspension was then deposited on the MALDI plates, allowed to dry, and subjected to MALDI-MS analysis. The MALDI-MS results showed that the acidic compounds (lauric and benzoic acids) mixed with UiO-66-NH_2 had lower signal intensity, as compared with their basic counterparts (pyridine and cytidine). The opposite results were observed when the same analytes were mixed with UiO-66-COOH. However, acidic compounds did have relatively higher signals when mixed with UiO-66 (Figure 6). These MALDI-MS data indicate that an acid/base chemistry transpires when proton exchange occurs. When the acid/base chemistry becomes stronger between the analyte and the MOF, their interaction requires higher energy, and thus, the MALDI-MS signal intensity becomes lower because of the higher energy needed to break the binding between the MOF and the analytes. Such energy may not be sufficient during the MALDI ionization step. The UiO-66 surface is considered acidic because of the presence of coordinated zirconium ions, which have been reported as a hard Lewis acid, with Zr(IV) having a pK_a = 0.22.[19,20] Overall, the surface modification of the MOFs affected the MALDI-MS response when acidic and basic compounds were analyzed with the mentioned MOFs. Such differences in acidic and basic properties of the

analytes, and to a lesser extent of the MOFs, were the major factors that affected their respective MALDI-MS responses. To support such postulates, we will use other MOFs that have clear differences in their acidic and basic properties to determine whether proton exchange among the mixtures of the MOFs and acidic and basic analytes is a dominant factor in determining the level of response during MALDI-MS analysis.

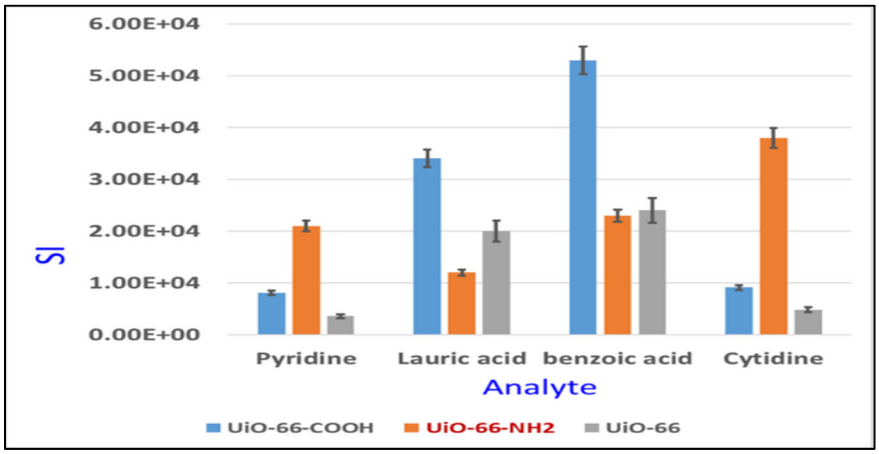

Figure 6. Comparative MALDI-MS response for UiO-66, UiO-66-COOH, and UiO-66-NH_2 mixed with pyridine, cytidine, lauric acid, and benzoic acid.

3.4 Effect of Metal Ions on the MOF Structures and MALDI-MS Analysis of Acidic and Basic Compounds

We examined the MALDI-MS ionization response for mixtures of the acidic and basic compounds with MOFs containing different metal ions coordinated in their SBU. The MOFs used were HKUST-1, which are also known as Cu_3(1,3,5-benzenetricarboxylate= BTC)$_2$/Cu–BTC, PCN-250, and PCN-250-Ni. The same acidic compounds were used in Section 3.3. Cu–BTC is a neutral coordination polymer that has dimeric cupric tetracarboxylate units and twelve carboxylate oxygen atoms from the two betacellulin (BTC) ligands bound to four coordination sites for each of the three Cu^{2+} ions.[22] These copper complex units form a face-centered crystal lattice. Cu–BTC has main pores of an approximately 0.9 nm diameter and forms a cubic network (Figure 7).

We also examined PCN MOFs, namely, PCN-250 and PCN-250-Ni. PCN-250 contained iron ions in its SBU, and it consists of six connected $Fe_2M(\mu_3–O)$ building blocks and rectangular tetratopic L22. The PCN-250 series of MOFs is very stable in various solvents. The pore size of its coordination channels ranges from 0.5 to 1.0 nm and consists of Zr_6 clusters linked by porphyrine ligands. Each Zr cluster is capped by m^3 OH groups and connected to eight porphyrin ligands. The PCN-250 MOFs showed great chemical stability in various solvents, including a solution of hydrochloric acid.[23–26]

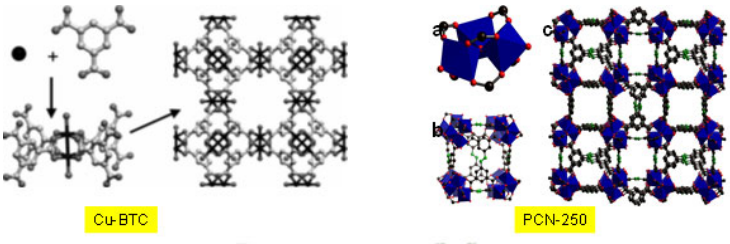

Figure 7. 3D structures of Cu–BTC and PCN-250 MOFs used in MALDI-MS analysis.

These MOF/analyte mixtures showed different MALDI-MS responses (Figure 8). The HKUST-1-acidic compound mixtures have higher MALDI-MS responses than those of the HKUST-1-basic mixtures. However, the basic analytes mixed with PCN-250-Ni have higher MALDI-MS responses than those of the PCN-250-Ni-acidic analyte mixtures. In fact, the acidic analytes mixed with PCN-250-Ni have negligible MALDI-MS responses as compared with their HKUST-1 and PCN-250 mixture counterparts. The trend in these MALDI-MS responses is not clear enough to draw a definite conclusion. Moreover, the acidic analytes had higher MALDI-MS responses when they were mixed with the PCN-250 MOF than with the PCN-250-benzoic acid mixture. Acidic analytes mixed with PCN-250 showed the highest MALDI-MS response as compared with the other MOF acidic and basic mixtures. Although the PCN-250 mixtures have better MALDI-MS responses with acidic compounds, the PCN-250/pyridine mixture also has a comparable MALDI-MS response to the PCN-250-acidic mixtures. This may not provide a definite conclusion regarding the impact of the presence of metal ions in the MOF structures and responses or contributions to acid/base chemistry during the MALDI-MS process. However, if Lewis acidity strength is considered as a factor, the Cu ions (HKUST–1) appear to be stronger Lewis acids than those of Fe ions (PCN-250). Ni ions (PCN-250-Ni) are the weakest Lewis acid.[27] If such factors have potential impact on the overall acid/base chemistry of the MOF, the resulting MALDI-MS analysis response should then, to a large extent, be similar to the one observed with UiO-66 MOFs (Figure 8).

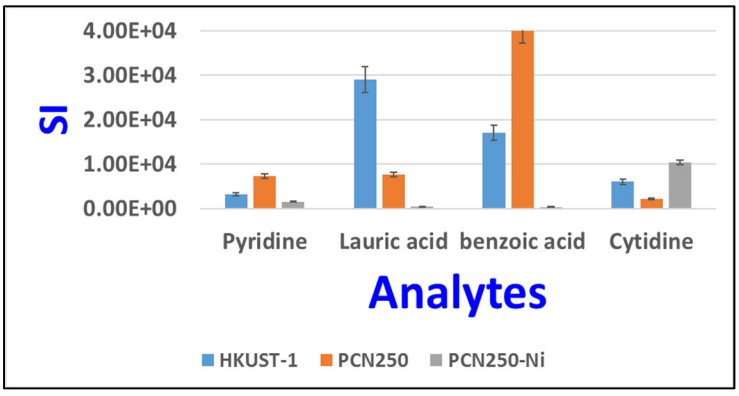

Figure 8. Comparative MALDI-MS responses for HKUST-1/Cu–BTC, PCN-250, and PCN-250-Ni mixed with pyridine, cytidine, lauric acid, and benzoic acid.

3.5 Stability of MOFs during MALDI-MS Analysis

The stability of the MALDI-MS response of the MOFs was investigated for MOF-545, MOF-545-Cu, PCN-250, and PCN-250-Ni. This set of experiments demonstrated that all of the MOFs were stable in their MALDI-MS signal responses with the same analyte mixtures. Although MOF-545 showed great variability, it did not diminish its instrumental response, and its high signal intensity was consistent, even after eight days of analyzing the same mixture. In addition, the signal intensity remained within the instrumental variance error. This increase in signal intensity for MOF-545 was not observed with the other MOFs or the conventional MALDI matrices, which could be caused by the increased residence time for the analyte molecules on MOF-545 that could be trapped inside the porous channel that have an equivalent size to that of the analyte. In addition, it could indicate that the binding of such an analyte with MOF-545 is kinetically driven (Figure 9).

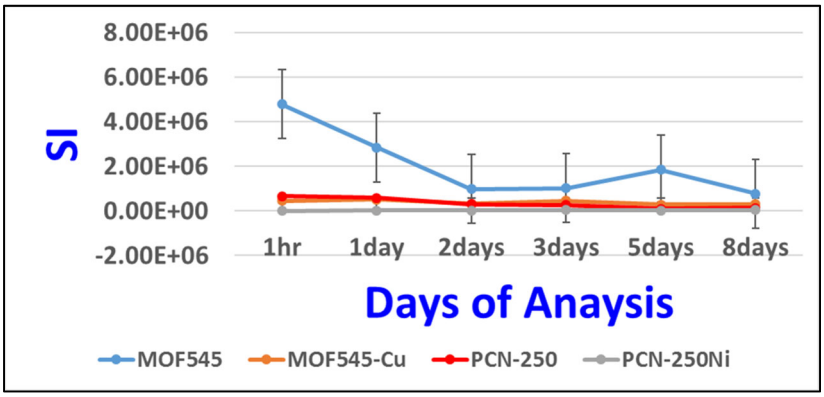

Figure 9. Reproducibility responses of MOF-545, MOF-545-Cu, PCN-250, and PCN-250-Ni during MALDI-MS process.

The other MOFs had similar responses and less variance than those of MOF-545. Too many factors may have contributed to this observation in the MALDI-MS analysis. Overall, the MALDI-MS response for the analyzed MOF/analyte mixtures indicates that, regardless of the analyte used in the mixture, reproducibility of the MOFs was evident for up to eight days of analyses. This is encouraging from the practical aspect of MOF use in MALDI analysis, as it is imperative to obtain reproducible responses using the same MOFs for repetitive runs. MOF reproducibility will reduce the consumption of matrix material, as is the case with conventional MALDI-MS matrices, and eventually, when bound to the MALDI plate surface as a film, it may result in more analyzed samples and an increased period of stability on the MALDI plate.

4. CONCLUSIONS

The experimental results showed that MOF substrates can be used to establish understanding of the ionization mechanism during the MALDI-MS process. Although more work is needed to confirm our findings, the preliminary data are useful for understanding the MALDI-MS ionization mechanism. The data can be used to design the most efficient MOF, which could act as a universal MALDI matrix. Clearly, an acid/base chemistry takes place between the MOFs and the acidic and basic analytes. This mechanism needs to be explored further to determine and recognize all the factors involved in an acid/base or proton exchange during the MOF/analyte MALDI-MS process. The MALDI response factor using different MOFs, such as Cu-BTC and MOF-545, showed significant improvement over the use of conventional MALDI matrices. There seem to be other factors that contribute to acid/base chemistry, such as functional groups on MOF surfaces, as seen in the UiO-66 series and the nature of the metal ions in the MOF structure (e.g., PCN-250 and Cu-BTC).

We are planning to better understand the ionization mechanism during the use of a MOF as a MALDI matrix. We will achieve this by choosing an additional set of analytes that offer similar bulk structures but with different functional groups that affect their respective acid/base properties. We will also investigate the impact of immobilized conventional MALDI matrices on MOFs and the effects of such binding on the MALDI ionization efficiency. The determination of the charge-transfer mechanism and its correlation with MALDI desorption is beneficial. This understanding will provide broader benefits to the use of MOFs in biocatalysis, biomimetics, and bioprocesses.

LITERATURE CITED

1. Rosinke, B.; Strupat, K.; Hillenkamp, F.; Rosenbusch, J.; Dencher, N.; Krüger, U.; Galla, H.J. Matrix-Assisted Laser Desorption/Ionization Mass Spectrometry (MALDI-MS) of Membrane Proteins and Non-Covalent Complexes. *J. Mass Spectrom.* **1995,** *30,* 1462–1468.

2. Cohen, S.L.; Chait, B.T. Influence of Matrix Solution Conditions on the MALDI-MS Analysis of Peptides and Proteins. *Anal. Chem.* **1996,** *68* (1), 31–37.

3. Fenselau, C.; Demirev, P.A. Characterization of Intact Microorganisms by MALDI Mass Spectrometry. *Mass Spectrom. Rev.* **2001,** *20* (4), 157–171.

4. Chaurand P.; Norris, J.L.; Cornett, D.S.; Mobley, J.A.; Caprioli, R.M. New Developments in Profiling and Imaging of Proteins from Tissue Sections by MALDI Mass Spectrometry. *J. Prot. Res*. **2006,** *5* (11), 2889–2900.

5. Tanaka, K.; Waki, H.; Ido, Y.; Akita, S.; Yoshida, Y.; Yoshida, T.; Matsuo, T. Protein and Polymer Analyses up to *m/z* 100,000 by Laser Ionization Time-of-Flight Mass Spectrometry. *Rapid Comm. Mass Spec.* **1988,** *2* (8), 151–153.

6. Demeure, K.; Quinton, L.; Gabelica, V.; De Pauw, E. Rational Selection of the Optimum MALDI Matrix for Top-Down Proteomics by in-Source Decay. *Anal. Chem.* **2007,** *79* (22), 8678–8685.

7. Cohen, S.L.; Chait, B.T. Influence of Matrix Solution Conditions on the MALDI-MS Analysis of Peptides and Proteins. *Anal. Chem.* **1996,** *68* (1), 31–37.

8. Dong, X.; Cheng, J.; Li, J.; Wang, Y. Graphene as a Novel Matrix for the Analysis of Small Molecules by MALDI-TOF MS. *Anal. Chem.* **2010,** *82* (14), 6208–6214.

9. Farha, O.K.; Yazaydın, A.Ö.; Eryazici, I.; Malliakas, C.D.; Hauser, B.G.; Kanatzidis, M.G.; Nguyen, S.T.; Snurr, R.Q.; Hu, J.T. De Novo Synthesis of a Metal–Organic Framework Material Featuring Ultrahigh Surface Area and Gas Storage Capacities. *Nat. Chem.* **2010,** *2* (11), 944–948.

10. Kaye, S.S.; Dailly, A.; Yaghi, O.M.; Long, J.R. Impact of Preparation and Handling on the Hydrogen Storage Properties of Zn^4O(1,4-Benzenedicarboxylate)^3 (MOF-5). *J. Am. Chem. Soc.* **2007,** *129* (46), 14176–14177.

11. Kreno, L.E.; Leong, K.; Farha, O.K.; Allendorf, M.; Van Duyne, R.P.; Hu, J.T. Metal–Organic Framework Materials as Chemical Sensors. *Chem. Rev.* **2012,** *112* (2), 1105–1125.

12. DeCoste, J.B.; Peterson, G.W. Metal-Organic Frameworks for Air Purification of Toxic Chemicals. *Chem. Rev.* **2014,** *114* (11), 5695–5727.

13. Lee, J.; Farha, O.K.; Roberts, J.; Scheidt, K.A.; Nguyen, S.T.; Hu, J.T. Metal–Organic Framework Materials as Catalysts. *Chem. Soc. Rev.* **2009,** *38* (5), 1450–1459.

14. Colaianni, S.M.; Nielsen, O.F. Low-Frequency Raman Spectroscopy. *J. Mol. Struct.* **1995,** *347,* 267–283.

15. Puretzky, A.A.; Liang, L.; Li, X.; Xiao, K.; Sumpter, B.G.; Meunier, V.; Geohegan, D.B. Twisted $MoSe_2$ Bilayers with Variable Local Stacking and Interlayer Coupling Revealed by Low-Frequency Raman Spectroscopy. *ACS Nano* **2016,** *10* (2), 2736–2744.

16. Ferrari, A.C.; Basko, D.M. Raman Spectroscopy as a Versatile Tool for Studying the Properties of Graphene. *Nat. Nano.* **2013,** *8* (4), 235–246.

17. Kirmess, K.M.; Knochenmuss, R.; Blanchard, G.J.; Kinsel, G.R. MALDI Ionization Mechanisms Investigated by Comparison of Isomers of Dihydroxybenzoic Acid. *J. Mass Spectrom.* **2016,** *51* (1), 79–85.

18. Knochenmuss, R. Ion Formation Mechanisms in UV-MALDI. *Analyst* **2006,** *131* (9), 966–986.

19. Wadas, T.J.; Wong, E.H.; Weisman, G.R.; Anderson, C.J. Coordinating Radiometals of Copper, Gallium, Indium, Yttrium, and Zirconium for PET and SPECT Imaging of Disease. *Chem Rev*. **2010,** *110* (5), 2858–2902.

20. Shih, Y.H.; Chien, C.H.; Singco, B.; Hsu, C.L.; Lin, C.H.; Huang, H.Y. Metal–Organic Frameworks: New Matrices for Surface-Assisted Laser Desorption–Ionization Mass Spectrometry. *Chem. Comm.* **2013,** *49* (43), 4929–4931.

21. Cavka, J.H.; Jakobsen, S.; Olsbye, U.; Guillou, N.; Lamberti, C.; Bordiga, S.; Lillerud, K.P. A New Zirconium Inorganic Building Brick Forming Metal Organic Frameworks with Exceptional Stability. *J. Am. Chem. Soc.* **2008,** *130* (42), 13850–13851.

22. An, J.; Farha, O.K.; Hu, J.T.; Pohl, E.; Yeh, J.I.; Rosi, N.L. Metal-Adeninate Vertices for the Construction of an Exceptionally Porous Metal-Organic Framework. *Nat. Comm.* **2012,** *3,* 604.

23. Morris, W.; Volosskiy, B.; Demir, S.; Gándara, F.; McGrier, P.L.; Furukawa, H.; Cascio, D.; Stoddart, J.F.; Yaghi, O.M. Synthesis, Structure, and Metalation of Two New Highly Porous Zirconium Metal–Organic Frameworks. *Inorg. Chem.* **2012,** *51* (12), 6443–6445.

24. Mondloch, J.E.; Bury, W.; Fairen-Jimenez, D.; Kwon, S.; DeMarco, E.J.; Weston, M.H.; Sarjeant, A.A.; Nguyen, S.T.; Stair, P.C.; Snurr, R.Q.; Farha, O.K. Vapor-Phase Metalation by Atomic Layer Deposition in a Metal-Organic Framework. *J. Am. Chem. Soc.* **2013,** *135* (28), 10294–10297.

25. Kandiah, M.; Nilsen, M.H.; Usseglio, S.; Jakobsen, S.; Olsbye, U.; Tilset, M.; Larabi, C.; Quadrelli, E.A.; Bonino, F.; Lillerud, K.P. Synthesis and Stability of Tagged-UiO-66 Zr MOFs. *Chem. Mat.* **2010,** *22* (24), 6632–6640.

26. Mondloch, J.E.; Karagiaridi, O.; Farha, O.K.; Hu, J.T. Activation of Metal-Organic Framework Materials. *Cryst. Eng. Comm.* **2013,** *15* (45), 9258–9264.

27. Lawrance, G.A. Reactions Involving the Metal Oxidation State. In *Introduction to Coordination Chemistry*. John Wiley & Sons, Ltd.: New York, 2010, p 191.

Blank

ACRONYMS AND ABBREVIATIONS

ACN	acetonitrile
BTC	betacellulin
BTC in MOF	1,3,5-benzenetricarboxylate
CA	cinnamic acid
CCD	charge-coupled device
HKUST-1	Hong Kong University of Science and Technology
LFRS	low-frequency Raman spectroscopy
MALDI	matrix-assisted laser desorption/ionization
MALDI-MS	MALDI-mass spectrometry
MeOH	methanol
MOF	metal-organic framework
MS	mass spectrometry
m/z	mass-to-charge ratio
PCN	poly-coordinated network
SA	sinapic acid
SBU	secondary building unit
TFA	trifluoroacetic acid
TOF	time of flight

DISTRIBUTION LIST

The following individuals and organizations were provided with one Adobe portable document format (pdf) electronic version of this report:

U.S. Army Edgewood Chemical
Biological Center (ECBC)
Detection Spectrometry Branch
RDCB-DRI-D
ATTN: Jabbour, R.
Wade, M.

ECBC Technical Library
RDCB-DRL
ATTN: Foppiano, S.
Stein, J.

ECBC CBR Filtration Branch
RDCB-DRP-F
ATTN: Peterson, G.
DeCoste, J.

Defense Technical Information Center
ATTN: DTIC OA


EDGEWOOD CHEMICAL BIOLOGICAL CENTER
A U.S. Army RDECOM Laboratory